

 Open access • Journal Article • DOI:10.1029/2018GL077706

## Tracking Groundwater Levels Using the Ambient Seismic Field — [Source link](#)

T. Clements, Marine A. Denolle

**Institutions:** Harvard University

**Published on:** 16 Jul 2018 - Geophysical Research Letters (John Wiley & Sons, Ltd)

**Topics:** Groundwater and Aquifer

Related papers:

- [Passive image interferometry and seasonal variations of seismic velocities at Merapi Volcano, Indonesia](#)
- [Postseismic Relaxation Along the San Andreas Fault at Parkfield from Continuous Seismological Observations](#)
- [Towards forecasting volcanic eruptions using seismic noise](#)
- [Seasonal Crustal Seismic Velocity Changes Throughout Japan](#)
- [Toward Forecasting Volcanic Eruptions using Seismic Noise](#)

Share this paper:    

View more about this paper here: <https://typeset.io/papers/tracking-groundwater-levels-using-the-ambient-seismic-field-1fh9wwgnqx>

# Tracking Groundwater Levels using the Ambient Seismic Field

Timothy Clements<sup>1</sup>, Marine A. Denolle<sup>1</sup>

<sup>1</sup>Department of Earth and Planetary Sciences, Harvard University, Cambridge, MA

## Key Points:

- Groundwater levels in the San Gabriel Valley Basin, California reach all-time low after 2011-2016 drought
- Seismic velocities respond linearly with drawdown and recharge of ground water aquifer
- Time-dependent maps of seismic velocity change yield high temporal and spatial resolution maps of groundwater levels

---

Corresponding author: Tim Clements, [thclements@g.harvard.edu](mailto:thclements@g.harvard.edu)

## Abstract

Aquifers are vital groundwater reservoirs for residential, agricultural, and industrial activities worldwide. Tracking their state with high temporal and spatial resolution is critical for water resource management at the regional scale yet is rarely achieved from a single dataset. Here, we show that variations in groundwater levels can be mapped using perturbations in seismic velocity ( $dv/v$ ). We recover daily measurements of  $dv/v$  in the San Gabriel Valley, California, from cross correlation of the ambient seismic field.  $dv/v$  reproduces the groundwater level changes that are marked by the multi-year depletions and rapid recharges typical of California's cycles of droughts and floods.  $dv/v$  correlates spatially with vertical surface displacements and deformation measured with GPS. Our results successfully predict the volume of water lost in the San Gabriel Valley during the 2012-2016 drought and thus provide a new approach to monitor groundwater storage.

## 1 Introduction

Groundwater supplies one third of the fresh water used for residential, agricultural, and industrial use in the world [Döll *et al.*, 2012]. With increasing demand, over-withdrawal of groundwater has led to subsidence and a loss of groundwater storage in numerous aquifers across the world [Galloway and Burbey, 2011]. This is especially problematic for more than two billion people worldwide that live farther than 5 km from a source of surface fresh water [Kummu *et al.*, 2011]. Compounding this is the role of climate change, which has led to more frequent and pronounced dry and hot years, along with stronger extreme precipitation events in places like California [Swain *et al.*, 2016; Teng and Branstator, 2017; Dettinger *et al.*, 2011]. Accurate monitoring of groundwater levels is required to manage water supplies, yet comprehensive groundwater level measurements on the local to global scales are lacking [Wada *et al.* [2010], especially in the context of climate change [Taylor *et al.*, 2012]. Surface displacements measured by GPS provide high temporal but sparse spatial resolution of groundwater level changes [Bawden *et al.*, 2001; King *et al.*, 2007; Ji and Herring, 2012], while those measured by Interferometric Synthetic-Aperture Radar (InSAR) bring high spatial resolution but limited temporal resolution [King *et al.*, 2007; Galloway and Hoffmann, 2007; Chaussard *et al.*, 2017]. Gravity measurements from the GRACE satellite are sensitive to water mass changes, but only at large wavelengths and they suffer non-uniqueness between water mass and aquifer depths [Rodell *et al.*, 2009; Xiao *et al.*, 2017].

The cross-correlation of ambient seismic time series [Shapiro and Campillo, 2004; Campillo, 2006] can remedy these issues by providing high spatial and temporal resolution of the change in bulk seismic velocity,  $dv/v$ , within a groundwater basin.  $dv/v$  has been widely used in recent years to study the dynamics of Earth's crust in response to earthquakes [Brennguier *et al.*, 2008a; Wegler *et al.*, 2009; Taira *et al.*, 2015], volcanic eruptions [Brennguier *et al.*, 2008b] and ice sheet melt [Mordret *et al.*, 2015]. Seasonal variations from precipitation [Sens-Schönfelder and Wegler, 2006; Meier *et al.*, 2010; Tsai, 2011; Wang *et al.*, 2017], air temperature changes [Meier *et al.*, 2010; Tsai, 2011; Hillers *et al.*, 2015], freeze-thaw of permafrost [James *et al.*, 2017] and long-term variations from climatic forcing [Lecocq *et al.*, 2017] are known to influence shallow seismic wavespeeds.  $dv/v$  is conducive to monitoring groundwater levels, as the velocity of seismic waves that scattered within water-saturated rocks is sensitive to changes in pore pressure [Grêt *et al.*, 2006]. Increasing pore pressure opens cracks and decreases the area of grain contacts, which in turns decreases seismic velocity [Christensen and Wang, 1985]. Seismic waves naturally scatter in the Earth and provide an averaged and volumetric sampling of the medium. This contrasts with measurements from a ground water well, which are sensitive to a specific location [Healy and Cook, 2002] that may not be representative of the aquifer if the permeability structure is heterogeneous.

This study presents the perturbations in bulk seismic velocity ( $dv/v$ ) in the San Gabriel Valley (SGV), Eastern Los Angeles County, California. The SGV contains three unconfined,

62 urban aquifers: the San Gabriel, the Puente, and the Raymond Basins. The east-northeast-  
 63 striking Raymond Fault acts as a barrier to flow between the Raymond and San Gabriel  
 64 Basins, while the San Gabriel and Puente Basins are hydraulically connected [*California*  
 65 *Department of Water Resources*, 1966; *Yeats*, 2004; *Main San Gabriel Watermaster*, 2017].  
 66 Water-bearing sediments reach a maximum thickness of 1,200 m in the central part of the  
 67 SGV [*California Department of Water Resources*, 1966]. The SGV Basin is recharged by a  
 68 combination of infiltration from rainfall, runoff from the San Gabriel Mountains, stormwa-  
 69 ter capture, and imported water from the State Water Project. During droughts, groundwa-  
 70 ter supplies over 40% of water demand in the SGV [*Main San Gabriel Watermaster*, 2017].  
 71 We consider changes in SGV groundwater in the period Jan 2000 - Jul 2017. This period  
 72 is notable for having three major droughts in southern California (2002-2004, 2007-2009,  
 73 and 2012-2016) [*California Department of Water Resources*, 2015]. During the most recent  
 74 drought, groundwater levels dropped 18 m in the SGV in the Baldwin Park Key Well (Fig.  
 75 1.), reaching all-time low levels in Oct 2016. Even with above average precipitation in the  
 76 winter of 2016-2017, groundwater levels have only recovered 1.7 m in the SGV basin due to  
 77 uptake by drought-parched soil [*Main San Gabriel Watermaster*, 2017].

## 78 2 Data and Methods

### 79 Ambient Seismic Cross-Correlation

80 We use continuous data from broad-band vertical component seismometers in the Cal-  
 81 ifornia Integrated Seismic Network (CI) from Jan 2000 - Jul 2017 (Fig 1.). All raw wave-  
 82 forms are downsampled to 20 Hz, demeaned, and detrended. We apply one-bit normalization  
 83 and whiten in the frequency domain from 0.05 to 4 Hz [*Bensen et al.*, 2007; *Lecocq et al.*,  
 84 2017]. Daily time series are segmented into 1-hour windows with 30 minutes of overlap be-  
 85 tween successive windows and cross-correlated using the MSNoise package [*Lecocq et al.*,  
 86 2014]. NCFs are computed for all station pairs in all available data ranges. Instrument cor-  
 87 rections are applied after cross-correlating. Hourly windows of raw data with maximum  
 88 absolute amplitude greater than ten times the standard deviation of the daily trace are dis-  
 89 carded. A daily NCF is formed by stacking all hourly NCFs from each day.

90 Daily changes in seismic velocity are computed using the Moving Window Cross-  
 91 Spectrum (MWCS) technique [*Poupinet et al.*, 1984; *Clarke et al.*, 2011]. This technique,  
 92 unlike the stretching technique of *Sens-Schönfelder and Wegler* [2006], does not assume a  
 93 global, linear time shift in phase arrival and is less susceptible to temporal variations in the  
 94 source of seismic noise [*Zhan et al.*, 2013]. We compute time shifts,  $dt$ , in the coda of daily  
 95 NCFs relative to a reference NCF, the stack of all NCFs for each station pair, in the 0.1 - 0.25  
 96 Hz and 0.5 - 2 Hz frequency bands. For each day, the previous 30 days of NCFs are stacked  
 97 to improve the stability of the MWCS analysis. Time shifts  $dt$  and coherency  $c$  between the  
 98 reference and daily NCF are calculated beginning after the 0.5 km/s arrival in the coda in  
 99 30 s windows for 0.1 - 0.25 Hz and 10 s windows for 0.5 - 2 Hz, shifted by 20% of the win-  
 100 dow length.  $dt$  measurements with time shift  $dt \leq 0.2$  s in each window and coherency  
 101  $c \geq 0.5$  are included. A daily time shift  $dt/t$  is measured by regressing time shifts  $dt$  from  
 102 each window in the causal and acausal part of the coda. Assuming that there is linear rela-  
 103 tion between relative time lags and that the velocity change is homogeneous throughout the  
 104 sampling medium, the daily velocity variation is just  $-dt/t = dv/v$ .

### 105 $dv/v$ Regionalization

106 We map  $dv/v$  spatially in 1220 m x 905 m grid cells in the 0.5 - 2.0 Hz frequency band  
 107 using the regionalization method of *Brenguier et al.* [2008b], which approximates the sensi-  
 108 tivity of each station pair as an ellipse.  $dv/v$  in all grid cells within 3 km of the straight line  
 109 path between each station pair are set as the difference in  $dv/v$  between the starting and end  
 110 date of the period of interest. We then average all grid cells over all station pairs. A gaussian  
 111 smoothing function has been applied to the  $dv/v$  maps in Fig 3. and 4. We did not use the

112 sensitivity kernels of *Obermann et al.* [2013] that assume homogeneous diffuse properties,  
 113 which are unlikely to be satisfied in resonating sedimentary basins.

## 114 2.1 Water Storage from $dv/v$ .

115 We calculate the change in groundwater storage  $dV_w$  in a particular region in the SGV  
 116 basin from  $dv/v$  using

$$dV_w = S_y A \Delta_{dv/v} \beta \quad (1)$$

117 where  $S_y$  is the specific yield,  $A$  is the area of a grid cell in the regionalization of  $dv/v$ ,  
 118  $\Delta_{dv/v}$  is the change in seismic velocity in a grid cell between two dates, and  $\beta$  is the ratio  
 119 of a unit change in hydraulic head,  $\Delta h$ , to a unit change in  $\Delta_{dv/v}$  [*Fitts*, 2013]. The prod-  
 120 uct  $\Delta_{dv/v} \beta = \Delta h$  gives the average change in hydraulic head in a grid cell.  $S_y$  varies from  
 121 0.03 to 0.24 across the SGV, with averages of 0.14, 0.08 and 0.09 in the central, eastern, and  
 122 western parts of the SGV, respectively [*California Department of Water Resources*, 1966].  
 123 We take  $S_y = 0.12$  as a representative, average value for the entire SGV basin. Assuming  
 124 that the inflation of the aquifer was totally elastic [*King et al.*, 2007], we use the 2005 rain  
 125 event (Jan 1 - Jun 1 2005) to calibrate  $\beta$  for the SGV. A 16.8 m increase in groundwater level  
 126 in the Key Well and -0.00125 (-0.125%) change in  $dv/v$  for the SGV basin gives a value of  
 127  $\beta = -13280 \frac{m}{\frac{m/s}{m/s}}$ . We find a similar negative value of  $\beta = -10900 \frac{m}{\frac{m/s}{m/s}}$  using the  $dv/v$   
 128 and groundwater level changes found by *Lecocq et al.* [2017]. We integrate  $dV_w$  over all grid  
 129 cells to get a total volume change within the SGV basin.

## 130 3 Results and Discussion

131 The  $dv/v$  variations we measure in the 0.5 - 2.0 Hz frequency range, which is greatly  
 132 sensitive to the upper 1,000 m of the basin, are the most promising for groundwater monitor-  
 133 ing at basin-scale [*Obermann et al.*, 2013]. The change in groundwater level in the Baldwin  
 134 Park Key Well explains most of the variance in the evolution of  $dv/v$  in the SGV. We observe  
 135 three distinct functional forms in our  $dv/v$  measurements : 1) seasonal periodicity, 2) impul-  
 136 sive events, and 3) multi-year linear trends (Fig 2.).

137 Seasonality in  $dv/v$  has been observed recently throughout Japan [*Wang et al.*, 2017],  
 138 where precipitation (snow or water), sea level changes, and thermal effects were identified  
 139 as probable mechanisms for seasonality in  $dv/v$ . Thermo-elastic strains were previously in-  
 140 voked to be responsible for seasonality in  $dv/v$  in the Los Angeles Basin from Jan 2001 - Jan  
 141 2004 [*Meier et al.*, 2010], and in some cases the greatest contributor to the seasonal signal in  
 142 the San Jacinto Fault area, California [*Hillers et al.*, 2015]. We use a thermo-elastic model  
 143 [*Tsai*, 2011] to remove seasonal  $dv/v$  due to surface temperature variations (Fig. 2.). We find  
 144 that seasonal thermo-elastic strains induce perturbations in wavespeed of about 0.03%, much  
 145 lower than the hydrological effects that perturb elastic wavespeeds that are about 0.15%. The  
 146 seasonal residual in  $dv/v$  we measure is thus a component of the seasonal recharge in ground-  
 147 water within the SGV basin [*Jasechko et al.*, 2014].

148 At the end of 2004, groundwater levels in the SGV were at an all-time low in the Bald-  
 149 win Park Key Well since measurements began in 1932. In contrast, the winter of 2004-2005  
 150 recorded the largest rainfall in a 100-year period in Los Angeles with 1 m of total precipi-  
 151 tation. Water levels in the Baldwin Park Key Well increased by over 16 m in a span of five  
 152 months. GPS stations recorded more than 40 mm of uplift in the central part of the SGV  
 153 [*King et al.*, 2007; *Ji and Herring*, 2012]. We find that  $dv/v$  decreased by 0.15% in the same  
 154 time frame. This impulsive drop in  $dv/v$  is similar to that seen after nearby earthquakes [*Bren-  
 155 guier et al.*, 2008a; *Wegler et al.*, 2009]. The largest decrease in  $dv/v$  is mapped in the center  
 156 of the SGV (Fig. 3), where the basin is deepest [*Yeats*, 2004], as were the largest deforma-  
 157 tions recorded with InSAR [*King et al.*, 2007]. There is no statistically significant phase lag

158 between the groundwater levels and  $dv/v$  response, suggesting a pure elastic response of  
159 the aquifer.

160  $dv/v$  due to groundwater level changes have been observed before [*Sens-Schönfelder*  
161 *and Wegler*, 2006], but not in the context of water resource management or drought. Re-  
162 cently, *Lecocq et al.* [2017] found that thermo-elastic strains, including those induced by  
163 long-term warming, and hydrologic loading contributed equally to  $dv/v$  over 30 years, due to  
164 relatively low fluctuations in groundwater levels, in the Grafenburg region, Germany. Here,  
165 the dominant process that impacts the variations in elastic wavespeed is the multi-year draw-  
166 down during periods of low precipitation [*Teng and Branstator*, 2017]. During the drought  
167 of 2012-2016, groundwater levels declined in the SGV at a rate of 450 mm/yr, which is one  
168 of the highest rates seen globally [*Wada et al.*, 2010]. The largest change in  $dv/v$  during the  
169 drought occurred at two stations located within the basin and atop the thickest part of the  
170 aquifer [*California Department of Water Resources*, 1966]. During the period Jan 2012- Jan  
171 2017, when additional well data is available throughout the SGV, we find spatial correlation  
172 between the change in  $dv/v$  and spatial and temporal patterns of groundwater change. The  
173 strongest increase of  $dv/v$  occurs in the south of the SGV (Fig. 4.). A small decrease in  $dv/v$   
174 during the same time frame suggests that the SGV and Raymond basins are hydraulically  
175 separated [*California Department of Water Resources*, 1966; *Ji and Herring*, 2012]. GPS  
176 stations during the same time period measured a contraction of the ground surface that may  
177 result from a elastic response of the basin.

178 The strong temporal correlation between groundwater levels in the Baldwin Park Key  
179 Well and  $dv/v$  (Fig. 2.) and spatial agreement between GPS displacements and well levels  
180 at key periods of time provide us confidence to map the change in groundwater level. We  
181 use the instantaneous elastic response of the 2005 rainfall event to calibrate the conversion  
182 between  $dv/v$  and groundwater level. Applying this calibration factor to the regionalization  
183 of  $dv/v$  from Jan 2012 - Jan 2017 yields a water storage loss of 0.48 km<sup>3</sup>. This matches well  
184 with the 0.45 - 0.5 km<sup>3</sup> of water that was pumped by from the main SGV Basin during the  
185 drought to meet water demand [*Main San Gabriel Watermaster*, 2017].

186 Our results imply that the change in seismic velocity,  $dv/v$ , has tremendous potential  
187 to monitor groundwater fluctuations in basins of moderate-size aquifers. Our analysis is able  
188 to provide the water volume change, at much higher spatial resolution than GRACE data. It  
189 has also the capabilities to provide a direct and continuous monitoring of the spatial varia-  
190 tions in ground water levels, bypassing the need to deploy multiple groundwater wells and  
191 performing GPS inversions.

## 192 **Acknowledgments**

193 Waveform data was accessed from the Southern California Earthquake Data Center (<https://doi.org/10.7914/SN/CI>).  
194 Groundwater data was accessed from the Los Angeles County Department of Public Works  
195 (<http://ladpw.org/wrd/>) and San Gabriel Watermaster (<http://www.watermaster.org/>). GPS  
196 time series data was accessed from NASA's Crustal Dynamics Data Information System  
197 ([ftp://cddis.gsfc.nasa.gov/pub/GPS\\_Explorer/latest/](ftp://cddis.gsfc.nasa.gov/pub/GPS_Explorer/latest/)). Weather data was accessed from  
198 the Western Regional Climate Center (<https://wrcc.dri.edu/>). The ObsPy, PyASDF, MPI4Py,  
199 SciPy ecosystem and MSNoise packages were used to process data. The computations in  
200 this paper were run on the Odyssey cluster supported by the FAS Division of Science, Re-  
201 search Computing Group at Harvard University. The authors would like to thank Loic Viens,  
202 Aurelien Mordret, Michel Campillo, Victor Tsai, and James Rice for thoughtful and helpful  
203 discussions. T.C. analyzed the data (seismic, ground water, GPS), created the figures, and  
204 wrote the manuscript. M.D. funded the research and edited the manuscript. M.D. and T.C.  
205 designed the project.

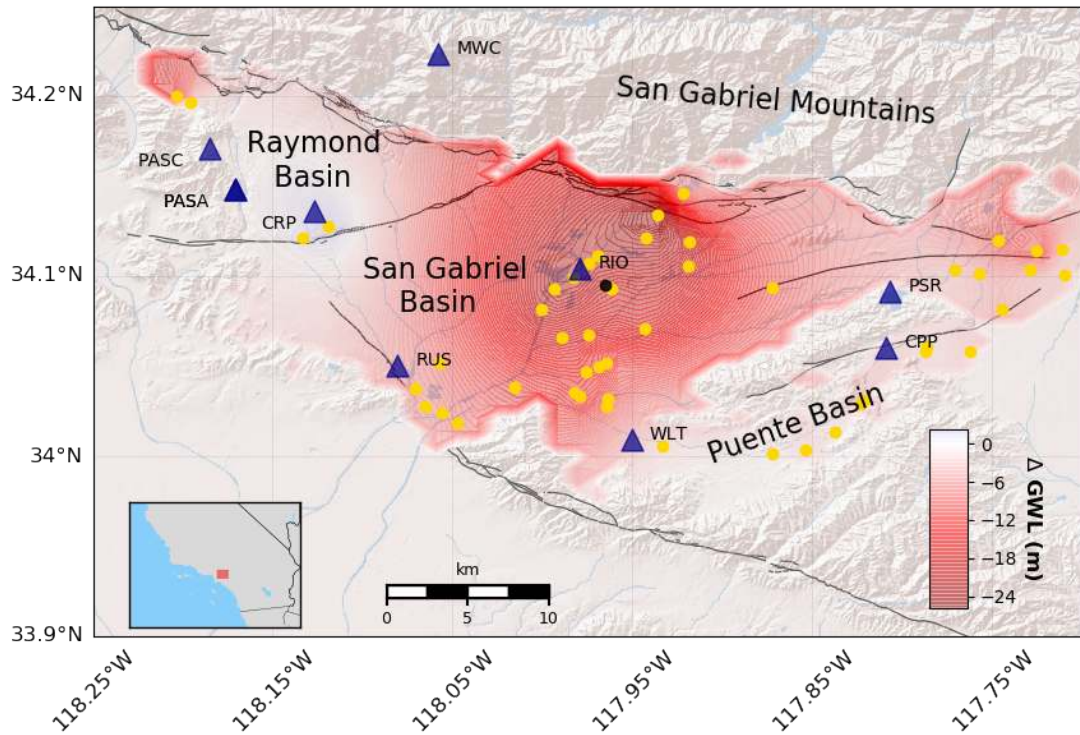
## References

- 206  
207 Bawden, G. W., W. Thatcher, R. S. Stein, K. W. Hudnut, and G. Peltzer (2001), Tectonic  
208 contraction across Los Angeles after removal of groundwater pumping effects, *Nature*,  
209 *412*(6849), 812–815, doi:10.1038/35090558.
- 210 Bensen, G. D., M. H. Ritzwoller, M. P. Barmin, A. L. Levshin, F. Lin, M. P. Moschetti, N. M.  
211 Shapiro, and Y. Yang (2007), Processing seismic ambient noise data to obtain reliable  
212 broad-band surface wave dispersion measurements, *Geophysical Journal International*,  
213 *169*(3), 1239–1260, doi:10.1111/j.1365-246X.2007.03374.x.
- 214 Brenguier, F., M. Campillo, C. Hadziioannou, N. M. Shapiro, R. M. Nadeau, and E. Larose  
215 (2008a), Postseismic Relaxation Along the, *Science*, *321*(September), 1478–1481, doi:  
216 10.1126/science.1160943.
- 217 Brenguier, F., N. Shapiro, M. Campillo, V. Ferrazzini, Z. Duputel, O. Coutant, and A. Ner-  
218 cessian (2008b), Towards forecasting volcanic eruptions using seismic noise, *Nature Geo-*  
219 *science*, *1*(2), 126–130, doi:10.1038/ngeo104.
- 220 California Department of Water Resources (1966), Planned utilization of ground water  
221 basins: San Gabriel Valley, *Tech. rep.*, Sacramento, California.
- 222 California Department of Water Resources (2015), California’s Most Significant Drought:  
223 Comparing Historical and Recent Conditions, *Tech. rep.*, Sacramento, California.
- 224 Campillo, M. (2006), Phase and correlation in ‘random’ seismic fields and the recon-  
225 struction of the green function, *Pure and Applied Geophysics*, *163*(2-3), 475–502, doi:  
226 10.1007/s00024-005-0032-8.
- 227 Chaussard, E., P. Milillo, R. Bürgmann, D. Perissin, E. J. Fielding, and B. Baker (2017),  
228 Remote Sensing of Ground Deformation for Monitoring Groundwater Manage-  
229 ment Practices: Application to the Santa Clara Valley During the 2012-2015 Cali-  
230 fornia Drought, *Journal of Geophysical Research: Solid Earth*, pp. 8566–8582, doi:  
231 10.1002/2017JB014676.
- 232 Christensen, N. I., and H. F. Wang (1985), Influence of pore pressure and confining pressure  
233 on dynamic elastic properties of Berea sandstone , doi:http://dx.doi.org/10.1016/0148-  
234 9062(86)90438-9.
- 235 Clarke, D., L. Zaccarelli, N. M. Shapiro, and F. Brenguier (2011), Assessment of resolution  
236 and accuracy of the Moving Window Cross Spectral technique for monitoring crustal tem-  
237 poral variations using ambient seismic noise, *Geophysical Journal International*, *186*(2),  
238 867–882, doi:10.1111/j.1365-246X.2011.05074.x.
- 239 Dettinger, M. D., F. M. Ralph, T. Das, P. J. Neiman, and D. R. Cayan (2011), Atmo-  
240 spheric Rivers, Floods and the Water Resources of California, *Water*, *3*(4), 445–478, doi:  
241 10.3390/w3020445.
- 242 Döll, P., H. Hoffmann-Dobrev, F. Portmann, S. Siebert, A. Eicker, M. Rodell, G. Strassberg,  
243 and B. Scanlon (2012), Impact of water withdrawals from groundwater and surface water  
244 on continental water storage variations, *Journal of Geodynamics*, *59-60*, 143–156, doi:  
245 10.1016/j.jog.2011.05.001.
- 246 Fitts, C. R. (2013), Groundwater, in *Groundwater Science*, pp. 1–22, Elsevier, doi:  
247 10.1016/B978-0-12-384705-8.00001-7.
- 248 Galloway, D. L., and T. J. Burbey (2011), Review: Regional land subsidence accompanying  
249 groundwater extraction, *Hydrogeology Journal*, *19*(8), 1459–1486, doi:10.1007/s10040-  
250 011-0775-5.
- 251 Galloway, D. L., and J. Hoffmann (2007), The application of satellite differential SAR  
252 interferometry-derived ground displacements in hydrogeology, *Hydrogeology Journal*,  
253 *15*(1), 133–154, doi:10.1007/s10040-006-0121-5.
- 254 Grêt, A., R. Snieder, and J. Scales (2006), Time-lapse monitoring of rock properties with  
255 coda wave interferometry, *Journal of Geophysical Research: Solid Earth*, *111*(3), 1–11,  
256 doi:10.1029/2004JB003354.
- 257 Healy, R. W., and P. G. Cook (2002), Using groundwater levels to estimate recharge, *Hydro-*  
258 *geology Journal*, *10*(1), 91–109, doi:10.1007/s10040-001-0178-0.

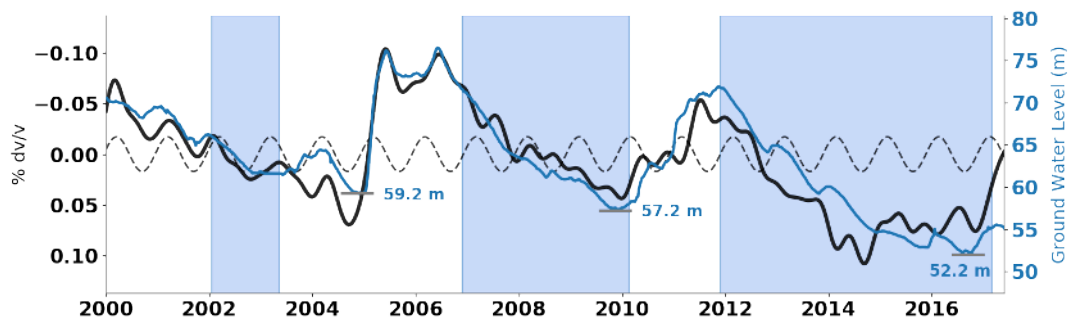
- 259 Hillers, G., Y. Ben-Zion, M. Campillo, and D. Zigone (2015), Seasonal variations of seismic  
 260 velocities in the San Jacinto fault area observed with ambient seismic noise, *Geophysical*  
 261 *Journal International*, 202(2), 920–932, doi:10.1093/gji/ggv151.
- 262 James, S. R., H. A. Knox, R. E. Abbott, and E. J. Sreaton (2017), Improved moving window  
 263 cross-spectral analysis for resolving large temporal seismic velocity changes in permafrost,  
 264 *Geophysical Research Letters*, 44(9), 4018–4026, doi:10.1002/2016GL072468.
- 265 Jasechko, S., S. J. Birks, T. Gleeson, Y. Wada, P. J. Fawcett, Z. D. Sharp, J. J. McDonnell,  
 266 and J. M. Welker (2014), The pronounced seasonality of global groundwater recharge,  
 267 *Water Resources Research*, 50(11), 8845–8867, doi:10.1002/2014WR015809.
- 268 Ji, K. H., and T. A. Herring (2012), Correlation between changes in groundwater levels and  
 269 surface deformation from GPS measurements in the San Gabriel Valley, California, *Geo-*  
 270 *physical Research Letters*, 39(1), 1–5, doi:10.1029/2011GL050195.
- 271 King, N. E., D. Argus, J. Langbein, D. C. Agnew, G. Bawden, R. S. Dollar, Z. Liu, D. Gal-  
 272 loway, E. Reichard, A. Yong, F. H. Webb, Y. Bock, K. Stark, and D. Barseghian (2007),  
 273 Space geodetic observation of expansion of the San Gabriel Valley, California, aquifer sys-  
 274 tem, during heavy rainfall in winter 2004–2005, *Journal of Geophysical Research: Solid*  
 275 *Earth*, 112(3), 1–11, doi:10.1029/2006JB004448.
- 276 Kumm, M., H. de Moel, P. J. Ward, and O. Varis (2011), How close do we live to wa-  
 277 ter? a global analysis of population distance to freshwater bodies, *PLoS ONE*, 6(6), doi:  
 278 10.1371/journal.pone.0020578.
- 279 Lecocq, T., C. Caudron, and F. Brenguier (2014), MSNoise, a Python Package for Moni-  
 280 toring Seismic Velocity Changes Using Ambient Seismic Noise, *Seismological Research*  
 281 *Letters*, 85(3), 715–726, doi:10.1785/0220130073.
- 282 Lecocq, T., L. Longuevergne, H. A. Pedersen, F. Brenguier, and K. Stammler (2017), Mon-  
 283 itoring ground water storage at mesoscale using seismic noise: 30 years of continuous  
 284 observation and thermo-elastic and hydrological modeling, *Scientific Reports*, 7(1), 1–16,  
 285 doi:10.1038/s41598-017-14468-9.
- 286 Main San Gabriel Watermaster (2017), 2016 - 2017 Annual Report, *Tech. rep.*, Azusa, Cali-  
 287 fornia.
- 288 Meier, U., N. M. Shapiro, and F. Brenguier (2010), Detecting seasonal variations in seismic  
 289 velocities within Los Angeles basin from correlations of ambient seismic noise, *Geophys-  
 290 ical Journal International*, 181(2), 985–996, doi:10.1111/j.1365-246X.2010.04550.x.
- 291 Mordret, A., T. D. Mikesell, C. Harig, B. P. Lipovsky, and A. Prieto (2015), Monitoring  
 292 South-West Greenland’s ice sheet melt with ambient seismic noise, *Science Advances*,  
 293 (May), 1–11, doi:10.1126/sciadv.1501538.
- 294 Obermann, A., T. Planès, E. Larose, C. Sens-Schönfelder, and M. Campillo (2013), Depth  
 295 sensitivity of seismic coda waves to velocity perturbations in an elastic heterogeneous  
 296 medium, *Geophysical Journal International*, 194(1), 372–382, doi:10.1093/gji/ggt043.
- 297 Poupinet, G., W. L. Ellsworth, and J. Frechet (1984), Monitoring velocity variations in the  
 298 crust using earthquake doublets: An application to the Calaveras Fault, California, *Journal*  
 299 *of Geophysical Research*, 89(B7), 5719, doi:10.1029/JB089iB07p05719.
- 300 Rodell, M., I. Velicogna, and J. S. Famiglietti (2009), Satellite-based estimates of groundwa-  
 301 ter depletion in India, *Nature*, 460(7258), 999–1002, doi:10.1038/nature08238.
- 302 Sens-Schönfelder, C., and U. Wegler (2006), Passive image interferometry and seasonal vari-  
 303 ations of seismic velocities at Merapi Volcano, Indonesia, *Geophysical Research Letters*,  
 304 33(21), 1–5, doi:10.1029/2006GL027797.
- 305 Shapiro, N. M., and M. Campillo (2004), Emergence of broadband Rayleigh waves from cor-  
 306 relations of the ambient seismic noise, *Geophysical Research Letters*, 31(7), 8–11, doi:  
 307 10.1029/2004GL019491.
- 308 Swain, D. L., D. E. Horton, D. L. Swain, D. E. Horton, D. Singh, and N. S. Diffenbaugh  
 309 (2016), Trends in atmospheric patterns conducive to seasonal precipitation and tempera-  
 310 ture extremes in California seasonal precipitation and temperature extremes, (April), 1–14,  
 311 doi:10.1126/sciadv.1501344.



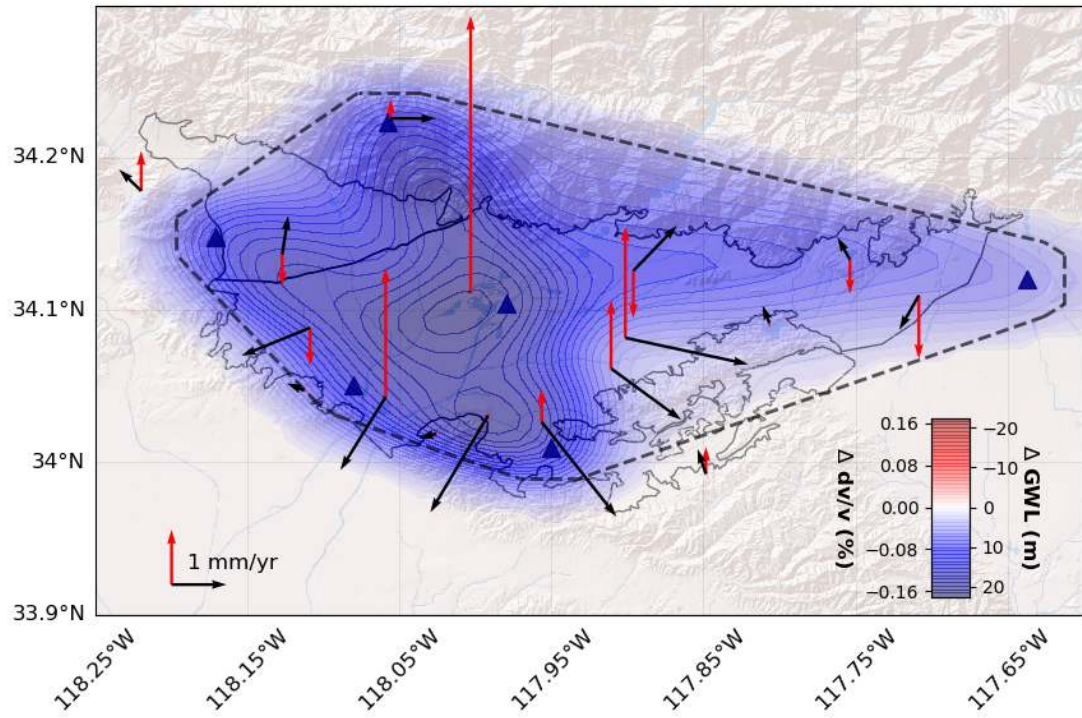
- 312 Taira, T., F. Brenguier, and Q. Kong (2015), Ambient noise-based monitoring of seismic  
313 velocity changes associated with the 2014 Mw 6.0 South Napa earthquake, (September  
314 2010), 6997–7004, doi:10.1002/2015GL065308.Received.
- 315 Taylor, R. G., B. Scanlon, P. Döll, M. Rodell, R. van Beek, Y. Wada, L. Longuev-  
316 ergne, M. Leblanc, J. S. Famiglietti, M. Edmunds, L. Konikow, T. R. Green, J. Chen,  
317 M. Taniguchi, M. F. P. Bierkens, A. MacDonald, Y. Fan, R. M. Maxwell, Y. Yechieli, J. J.  
318 Gurdak, D. M. Allen, M. Shamsudduha, K. Hiscock, P. J.-F. Yeh, I. Holman, and H. Trei-  
319 del (2012), Ground water and climate change, *Nature Climate Change*, 3(4), 322–329,  
320 doi:10.1038/nclimate1744.
- 321 Teng, H., and G. Branstator (2017), Causes of extreme ridges that induce california droughts,  
322 *Journal of Climate*, 30(4), 1477–1492, doi:10.1175/JCLI-D-16-0524.1.
- 323 Tsai, V. C. (2011), A model for seasonal changes in GPS positions and seismic wave speeds  
324 due to thermoelastic and hydrologic variations, *Journal of Geophysical Research: Solid*  
325 *Earth*, 116(4), 1–9, doi:10.1029/2010JB008156.
- 326 Wada, Y., L. P. Van Beek, C. M. Van Kempen, J. W. Reckman, S. Vasak, and M. F. Bierkens  
327 (2010), Global depletion of groundwater resources, *Geophysical Research Letters*, 37(20),  
328 1–5, doi:10.1029/2010GL044571.
- 329 Wang, Q. Y., F. Brenguier, M. Campillo, A. Lecointre, T. Takeda, and Y. Aoki (2017), Sea-  
330 sonal Crustal Seismic Velocity Changes Throughout Japan, *Journal of Geophysical Re-*  
331 *search: Solid Earth*, 122(10), 7987–8002, doi:10.1002/2017JB014307.
- 332 Wegler, U., H. Nakahara, C. Sens-Schönfelder, M. Korn, and K. Shiomi (2009), Sudden drop  
333 of seismic velocity after the 2004 Mw 6.6 mid-Niigata earthquake, Japan, observed with  
334 Passive Image Interferometry B06305, *Journal of Geophysical Research: Solid Earth*,  
335 114(6), 1–11, doi:10.1029/2008JB005869.
- 336 Xiao, M., A. Koppa, Z. Mekonnen, B. R. Pagán, S. Zhan, Q. Cao, A. Aierken, H. Lee,  
337 and D. P. Lettenmaier (2017), How much groundwater did California’s Central Val-  
338 ley lose during the 2012-2016 drought?, *Geophysical Research Letters*, pp. 1–8, doi:  
339 10.1002/2017GL073333.
- 340 Yeats, R. S. (2004), Tectonics of the san gabriel basin and surroundings, Southern Cal-  
341 ifornia, *Bulletin of the Geological Society of America*, 116(9-10), 1158–1182, doi:  
342 10.1130/B25346.1.
- 343 Zhan, Z., V. C. Tsai, and R. W. Clayton (2013), Spurious velocity changes caused by tem-  
344 poral variations in ambient noise frequency content, *Geophysical Journal International*,  
345 194(3), 1574–1581, doi:10.1093/gji/ggt170.



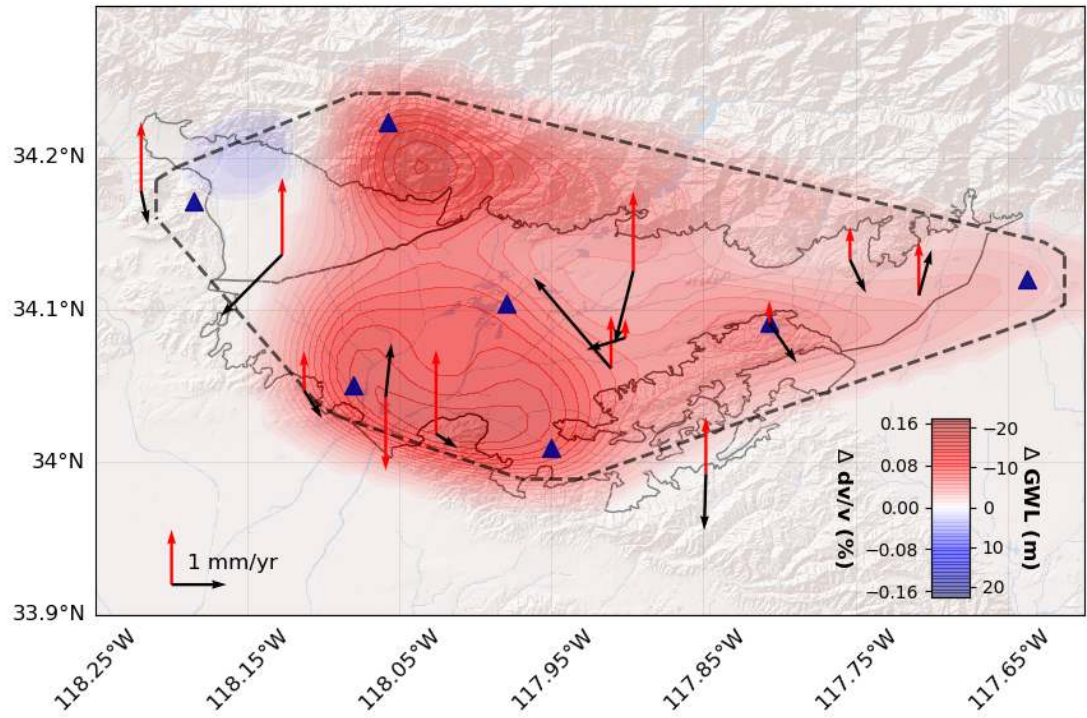
346 **Figure 1.** Groundwater level change in San Gabriel Valley during most recent drought (Fall 2012 - Fall  
 347 2016). Seismic stations are shown as blue triangles, and groundwater wells are shown as yellow circles. Black  
 348 circle indicates the position of the Baldwin Park Key well.



349 **Figure 2.** Relating seismic wavespeed temporal perturbation to ground water levels. Observed  $dv/v$  stacked  
 350 over all station pairs (black) with modeled  $dv/v$  due to thermo-elastic strain (dashed) removed compared with  
 351 ground water change (blue) in the Baldwin Park Key Well. Grey bars indicate lowest historical water levels of  
 352 the Baldwin Park Key Well. Blue patches indicate times of drought.



353 **Figure 3.**  $dv/v$  and GPS measurements after the 2005 Rain Event. Regionalization of  $dv/v$  changes Jan 2005  
 354 - Jun 2005 following large precipitation event in the SGV. GPS stations (red = vertical, black = horizontal)  
 355 uplift and move away from center of aquifer. The dashed black lines indicate extent of ray coverage. Scaling  
 356 of  $dv/v$  and groundwater level is from 2005 rain event.



357 **Figure 4.**  $dv/v$  and GPS measurements after 2012-2016 Drought. Regionalization of  $dv/v$  changes (Jan  
 358 2012- Jan 2017) during California's worst drought. GPS stations move toward center of aquifer. Symbols are  
 359 same as in Fig. 3.